Air Entrainment by a Viscous Jet Plunging into a Bath

Élise Lorenceau and David Quéré
Physique de la Matière Condensée, UMR 7125 du CNRS, Collège de France, Paris, France

Jens Eggers
School of Mathematics, University of Bristol, University Walk, Bristol BS8 1TW, United Kingdom
(Received 16 February 2004; published 13 December 2004)

A liquid jet plunging into a container of liquid often entrains a thin film of air with it, producing bubbles. This bubble production is detrimental to many industrial processes, such as filling a container with a molten glass or polymer, or in coating processes. Conversely, in making a foam, one uses this effect; hence it is important to control the rate of bubble production. Here, we measure the amount of air entrained by a viscous jet over a wide range of parameters and explain the phenomenon theoretically. Simple scaling arguments are shown to predict entrainment rates over 4 orders of magnitude in the dimensionless jet speed.

DOI: 10.1103/PhysRevLett.93.254501 PACS numbers: 47.15.Rq, 47.55.Dz, 47.85.–g

Air entrainment is a common phenomenon that can be encountered in many environmental situations, such as in breaking waves or steep chutes which contributes to river oxygenation, or in various industrial processes, such as aeration of water in open channels, coating processes, or the pouring of liquids. A paradigm for air entrainment is a jet plunging into a bath of fluid. If the fluid viscosity is small (e.g., water) [1–3], air entrainment occurs only if it is provoked by perturbing the jet. If the viscosity is higher (100 times that of water or more) [4,5], air entrainment occurs *spontaneously* by producing an air film. Here we present the first experimental measurements of entrainment rates and explain the results theoretically.

As described in [4–8], the liquid-air interface is hollowed by the flow of the plunging jet and a dip is formed around the fluid stream. Such a profile, which is continuous as long as the velocity V of the jet is constant, can be seen in Fig. 1(a). Something more dramatic happens if V increases above a threshold value V_c. The stationary profile ceases to exist, and a film of air is entrained with the jet into the bath. This gaseous film, which wraps around the liquid jet, decays into air bubbles a few centimeters below the surface [9]. This phenomenon is of tremendous practical importance: in many industrial processes a viscous liquid (typically molten glass, metal, or polymer) is poured inside a mold and the formation of bubbles damages the quality of the molded object.

Previous studies have focused on the threshold velocity V_c below which no air is entrained. At speeds close to V_c the interface at the bottom of the hollow region is very close to a cusp [see the circled zone of Fig. 1(a)]. Such singular features of free surfaces were first reported by Joseph *et al.* [10] and analyzed theoretically by Jeong and Moffatt [11], who found that a local balance between viscosity η and surface tension γ produces curvatures which increase exponentially with the capillary number $Ca = \eta V/\gamma$.

Any increase in jet velocity leads to a large decrease of the radius of curvature at the tip of the cusp. As pointed out in [6], this eventually results in the destruction of this tip: the upper fluid (usually air, of viscosity η_0) is forced into the tip and back out again by the external flow, and thus exerts a lubrication pressure on it. Below a critical tip radius (thus above a critical jet velocity), the tip "cracks" and a thin film of the upper fluid (often air) is entrained inside the bath [4,12,13]. In [6] it was shown that this critical tip radius increases with η_0/η, which together with Moffatt's law for the critical radius yields a threshold velocity $V_c \propto \ln(\eta/\eta_0)$, as was recently confirmed experimentally [7,8].

Just below V_c, we experimentally find the depth L of the region hollowed by the jet [cf. Fig. 2(a)] to be about 1 cm, several times the capillary length. This agrees with the estimate of $L \approx \sqrt{\eta V_c/\rho g}$, which follows from balancing viscous forces with gravity [7]. The surface deformation as measured by L thus far exceeds the capillary length $\kappa^{-1} = \sqrt{\gamma/\rho g}$, which results from a capillary-gravity balance.

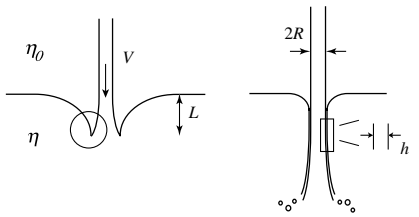

FIG. 1. Experimental setup. A cylindrical liquid jet of viscosity η surrounded by a fluid medium of viscosity η_0 plunges into a bath of the same liquid. The diameter of the jet is between 1.5 and 5 mm. On the left, the velocity of the jet is below the threshold velocity, and, on the right, it is above; hence the jet entrains an air film of thickness h into the bath.

The temporal development of the air film displayed in Fig. 2 indeed illustrates these different features. A jet 1.5 mm in diameter (about 1000 times more viscous than water) plunges into a bath of the same liquid. The jet velocity is controlled by the height of the reservoir from which the jet is formed. It is measured with a fast camera by following the motion of particles inserted randomly into the jet. Right above the interface, the velocity profile was observed to be a plug flow. In Fig. 2(a), the jet velocity is below the velocity of entrainment ($V < V_c$); hence the profile observed is stationary. The height of the reservoir, and therefore the velocity of the jet, is slightly increased between panel 2(a) and panel 2(b). This rise has a dramatic effect: the interface breaks and the jet entrains with it a thin air film (looking black because of light reflection). Its length grows from panel 2(b) to panel 2(f), where it reaches its final stationary trumpet shape. This shape is expected since the jet slows down as it enters the bath, and conservation of mass implies a gradual increase in radius (from which we can deduce the jet velocity as it penetrates the bath). At a certain depth (of several centimeters), the film decays into bubbles that are then driven upward and burst when they reach the surface. Note the velocity of the jet remains constant from panel 2(b) to panel 2(f).

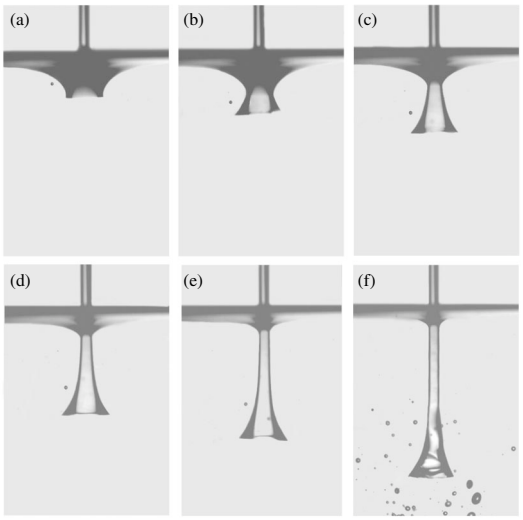

FIG. 2. A jet of viscous liquid (here silicone oil of viscosity $\eta = 970$ mPa s) and diameter 1.5 mm impinging on a bath of the same liquid. (a) Below a threshold velocity, the jet hollows the bath surface to a depth L, which increases with jet velocity up to a value of about 1 cm. (b)–(e) Above this threshold, air is entrained with the jet and (f) forms a stationary trumpetlike shape. At the same time, the surface of the bath around the jet relaxes to the shape of a static nonwetting meniscus, whose size is in the order of millimeters. The interval between two successive pictures is 130 ms. Note that the black line at the edge of the jet is no indication of the film thickness; it is due to the reflection of light by the curved air film of lower index of refraction.

The formation of the new stationary state [panel 2(f)] is accompanied by a considerable reduction in surface deformation of the bath. This is because the air film now "lubricates" the entry of the fluid jet, and shear stresses both inside the jet and in the liquid bath are greatly reduced. Instead, the shape of the bath surface close to the jet is now set by a purely *static* balance of gravity and surface tension forces, as confirmed by our measurements of the interface shape presented in Fig. 3. We superimpose profiles of the final shape [cf. Fig. 2(f)] corresponding to different jet velocities and compare them in Fig. 3 to the shape of a static meniscus drawn in full line in this figure. The latter is obtained by integrating the Laplace equation $\gamma C = \rho g z$ (C is the interface curvature) twice, assuming a "contact angle" of 180° with the air film and a flat profile for $z = 0$. The remarkable consequence of this observation is that for $\eta \gg \eta_0$ the fluid viscosity η becomes inconsequential, and the rate of air entrainment is determined by the speed of the jet and the viscosity of the entrained fluid η_0 alone.

Accordingly, we measured the variation of the film thickness h with jet speed for different values of η_0. In the case of oil films (between 10 and 30 times the viscosity of water) in a glycerol bath, the film thickness could be measured optically. To measure the thickness of the film of air (a few microns), we determined the total volume of the air bubbles being formed, thus giving the flow rate of air. Knowing the mean velocity of the air film, i.e., half the velocity of the jet, and the radius of the jet R, we can deduce the thickness of the film. Note that we measure R close to the surface, where it is very nearly constant, indicating that the jet speed is also constant and equal to the original jet velocity.

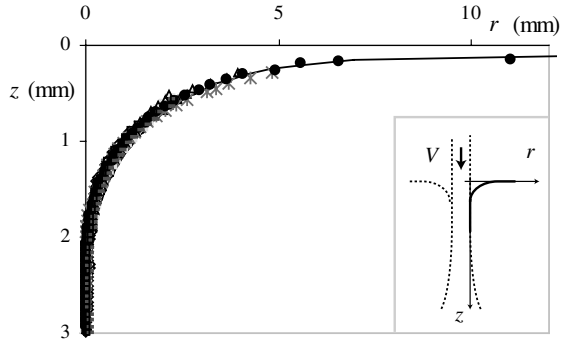

FIG. 3. Profile of the interface between the bath and the film of air, deduced from photographs such as Fig. 2(f), shown as the black line in the inset. The depth of the meniscus is plotted as a function of the radial position, and only the upper part where the trumpet joins the rest of the bath is shown. The different data points correspond to different jet velocities (all above the threshold velocity of air entrainment), between 0.7 and 2.2 m/s. The corresponding jet diameters are between 3.5 and 5.2 mm. All the data collapse onto the solid line, the static profile of a nonwetting meniscus.

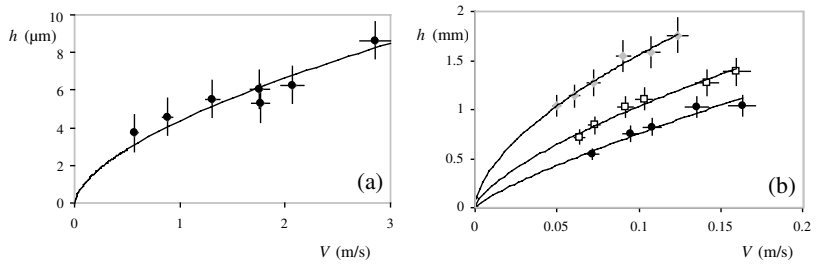

FIG. 4. Thickness of the film entrained by a glycerol jet ($\eta = 900$ mPa s) impacting a bath of glycerol. (a) Air film ($\eta_0 = 2 \times 10^{-2}$ mPa s), obtained with jets of diameter between 1.5 and 1.6 mm. (b) Oil films (the black, white, and gray symbols designate silicone oils of respective viscosity $\eta_0 = 8$, 20, and 32 mPa s), obtained by the impact of a glycerol sheet surrounded by oil. Note the difference in thickness between both cases. The fits are scaling laws of the form V^α, giving in both cases $\alpha = 0.7 \pm 0.1$.

We find that, for a given liquid-liquid or gas-liquid system, the film thickness increases with the jet velocity as a power law V^α, best fits giving $\alpha = 0.7 \pm 0.1$ (cf. Fig. 4). In fact, using a simple scaling argument based on our previous observations, we are able to quantitatively describe *all* our data. Namely, the film is sustained by the interplay between surface tension forces in the outer meniscus (which oppose the film's formation) and the viscous forces inside the thin film (which are responsible for entrainment). Equating pressure *gradients* at the junction between the static meniscus and the film, we obtain

$$\kappa\gamma/\lambda \approx \eta_0 V/h^2.$$

On the right-hand side appears the classical expression for the lubrication pressure gradient [14] based on the film's viscosity η_0, on the left-hand side, the gradient of curvature. To estimate the latter, we introduced a typical length scale λ over which the film thickness is varying in the matching region. To determine λ, we observe that the curvature of the film and of the static meniscus must match, yielding

$$\kappa \approx h/\lambda^2.$$

Combining both equations yields our central result:

$$h \approx \kappa^{-1}(\eta_0 V/\gamma)^{2/3}. \quad (1)$$

The predictive power of this expression is best appreciated by summarizing our data for different upper viscosities η_0 using the appropriate capillary number $Ca_0 = \eta_0 V/\gamma$. As shown in Fig. 5, Eq. (1) correctly predicts the $Ca_0^{2/3}$ behavior over 4 orders of magnitude in the capillary number and for a variety of different fluid-fluid and air-fluid systems. The straight line of Fig. 5 represents Eq. (1), including a prefactor 0.5 ± 0.2 which has been fitted to the data.

It has not escaped our notice that the arguments leading to (1) are the same used to derive the well-known Landau-Levich law [15,16] for the thickness of the *fluid* film entrained on a *solid* plate or fiber being withdrawn from a bath of viscous liquid [17]. In that case, the prefactor of Eq. (1) has been calculated and found equal to 0.9. Quite surprisingly, very similar arguments still apply in our case, but with the liquid jet assuming the role of the solid plate and the air the role of the viscous fluid. The reason is that the air film serves to isolate the jet from the rest of the fluid, such that the viscous fluid no longer plays a dynamical role, but just supplies the boundary conditions.

In fact, the boundary conditions that apply here are slightly different from those of the classical Landau-Levich problem. Namely, the outer boundary condition for the film now is that of a deformable solid, which changes the prefactors but not the scaling laws. Schwartz *et al.* [18] showed that a solidlike boundary thickens the entrained film (by a factor of $2^{2/3}$), which physically is due to the increased resistance of the capillary backflow, making it less efficient than in the presence of a free boundary. Combining the prefactor of 0.9 given by the classical Landau-Levich law and the correction cited above gives a prefactor of 1.4 for Eq. (1), which is 3 times larger than the one we found experimentally.

The change in boundary condition toward that of a solid also affects the flux of entrained matter: since the flow in the entrained film has a Couette profile (instead of

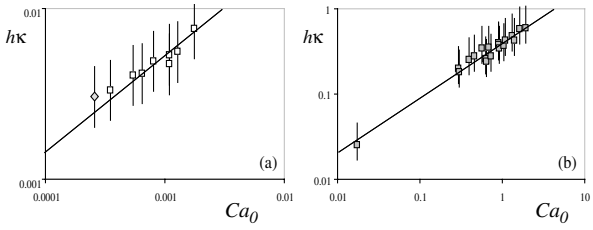

FIG. 5. (a) Thickness of the air film entrained by a glycerol jet (of diameter 1.5 mm) impacting a glycerol bath (open squares; the diamond is obtained using a silicone oil of same viscosity yet different surface tension as glycerol). (b) Thickness of oil films (solid symbols) entrained by a glycerol sheet surrounded by oil, impacting a glycerol bath. The thickness is normalized by the capillary length and plotted in logarithmic scales as a function of the capillary number $Ca_0 = \eta_0 V/\gamma$. The data are fitted by a straight line corresponding to Eq. (1), with prefactor 0.5 ± 0.2.

being a plug flow, as in a classical Landau-Levich film), we find $Q = 2\pi RhV/2$ for the flux, denoting the jet radius as R. Thus the flow of air depends strongly (as $V^{5/3}$) on the velocity, as suggested by everyday experience: we all know that the injection of air into an egg white is considerably enhanced by using a (fast) beater rather than a fork.

Figure 5(b) shows that (1) still describes our data for capillary numbers approaching unity, which can be understood by an argument proposed by Derjaguin [14]. For Ca_0 larger than unity, the meniscus is no longer quasistatic, but deformed by the flow, and gravity (instead of surface tension) becomes the force opposing entrainment. Balancing gravity $\Delta\rho g$ with the viscous force $\eta_0 V/h^2$ immediately yields $h \sim \kappa^{-1}(\eta_0 V/\gamma)^{1/2}$ as the entrainment law at large capillary number. This slight difference in exponent (1/2 instead of 2/3) implies a gradual transition toward another scaling law for large Ca_0, with relatively small corrections to (1) for $Ca_0 < 1$.

However, we do note that the high capillary number data fall below the line given by (1), which is probably the result of the transition toward the new power law. Fitting the prefactor only to the low capillary number data (Fig. 5(a)) would increase it and bring it closer to the theoretical prediction. The origin of the remaining discrepancy in the prefactor may be related to the fineness of the jet: Figure 5(a) is obtained with jets of diameter $2R \sim 1.5$ mm, so that we expect that the antagonist curvature of the jet tends to thin the film (because of its positive Laplace pressure). This does not modify the variation in $Ca_0^{2/3}$, but yields a correction in the prefactor in Eq. (1) scaling as $R\kappa$, which is of the order of 0.34 in the experiments displayed in Fig. 5(a).

Our results might be relevant to both the making of foams, as well as for the understanding of the way emulsions form. The main remaining obstacle is to elucidate the role of surfactants in both processes, which is the next step in our research program. We also expect that the rate of air entrained by solids plunging into a viscous bath—which, to the best of our knowledge, has never been explained—should be given by the same arguments, the air film similarly allowing a decoupling between the moving solid and the quiescent bath.

Note finally that a similar phenomenology is observed in a variety of situations where entrainment is forced externally, for example, by a rotating cylinder [10]. Another example consists in extracting the upper liquid from a two-fluid interface through a pipette (selective withdrawal) [19]. Above a threshold velocity, a very thin stream of the lower liquid is extracted as well. However, in these cases there is no decoupling between the extracted liquid and the quiescent bath, so our reasoning does not apply. Instead, an alternative scaling theory was recently put forward for selective withdrawal [20].

In conclusion, we have presented a unifying picture for the rate of air entrainment into a viscous fluid, by impacting both jets and solids. The rate depends strongly on the jet velocity, while the fluid viscosity is unimportant. A number of related entrainment phenomena remain to be understood.

We thank Frédéric Restagno, Frédéric Chevy, Alain Cartellier, and Etienne Reyssat for very valuable discussions and suggestions.

[1] Y. Zhu, H. N. Ogũz, and A. Prosperetti, J. Fluid Mech. **404**, 151 (2000).
[2] C. D. Ohl, H. N. Ogũz, and A. Prosperetti, Phys. Fluids **12**, 1710 (2000).
[3] B. Kersten, C. D. Ohl, and A. Prosperetti, Phys. Fluids **15**, 821 (2003).
[4] T. Lin and H. Donelly, AIChE J. **12**, 563 (1981).
[5] A. K. Bin, Chem. Eng. Sci. **48**, 3585 (1993).
[6] J. Eggers, Phys. Rev. Lett. **86**, 4290 (2001).
[7] E. Lorenceau, F. Restagno, and D. Quéré, Phys. Rev. Lett. **90**, 184501 (2003).
[8] A. Cartellier and J. Lasheras, Proceedings of the 3rd European-Japanese Two-Phase Flow Group Meeting, Certosa di Pontignano, Italy, edited by G. P. Celata, A. Tomiyama, I. Zun and P. di Marco.
[9] C. Clanet and J. Lasheras, Phys. Fluids **9**, 1864 (1997).
[10] D. Joseph, J. Nelson, M. Renardy, and Y. Renardy, J. Fluid Mech. **223**, 383 (1991).
[11] J.-T. Jeong and H. K. Moffatt, J. Fluid Mech. **241**, 1 (1992).
[12] P. G. Simpkins and V. Kuck, Nature (London) **403**, 641 (2000).
[13] S. Thoroddsen and Y.-K. Tan, Phys. Fluids **16**, L13 (2004).
[14] B. Derjaguin and S. Levi, *Film Coating Theory* (The Focal Press, London, 1964).
[15] L. Landau and V. Levich, Acta Physicochimica USSR **17**, 42 (1942).
[16] B. Derjaguin, Dokl. Acad. Sci. USSR **39**, 13 (1943).
[17] A. Linan [(unpublished)] has made the same observation.
[18] L. Schwartz, H. Princen, and A. Kiss, J. Fluid Mech. **172**, 259 (1986).
[19] I. Cohen and S. R. Nagel, Phys. Rev. Lett. **88**, 074501 (2002).
[20] W. W. Zhang, Phys. Rev. Lett. **93**, 184502 (2004).